Response to Anonymous Referee #3

The referee's comments are bolded and italicized while our comments are in plain text

The present work extends the knowledge on depositional and immersion mode freezing of ice on volcanic ash samples. Three selected ash samples have been chosen to study IN formation by Raman micro-spectroscopy. These samples cover the range of basaltic, andesitic and rhyolitic ash. While all three samples exhibit a similar behavior during depositional freezing, the authors claim varying behaviour during immersion mode freezing, which might be related to differences in the mineralogy of crystalline material. In contrast to previous studies, their results indicate, that a 'simple' parameterization of the immersion mode freezing for volcanic ashes is not legal. After a brief and straightforward introduction, a detailed experimental section is following. The results of their study are presented according to IN properties in the depositional and immersion mode. The paper concludes with a discussion on atmospheric implications. The paper is well written and could be interesting to the readership of Atmospheric Chemistry and Physics. However, the paper lacks of experimental details and interpretation of data obtained from Raman spectroscopy. Further, the significance of the results has to be discussed related to the limited dataset. Therefore, publication in ACP can only be considered after addressing the following major remarks in detail.

The author's would first like to thank anonymous referee #3 for his/her insightful comments that have improved the clarity of this manuscript

Major issues:

****) The title of the paper includes ". . . using Raman spectroscopy" – however, only Raman spectra related to depositional freezing are shown in figure 1. The authors claim, that their study is the first immersion mode freezing study, therefore it is absolutely important to discuss and display details of Raman spectra obtained during the immersion mode experiments in detail. Even experimental details have to be discussed like influence of laser power on heating of the droplets and disturbing the measurements and results. Further, for confocal Raman microscopy, height of the z-resolution must be discussed related to the sample size and height. How reliable are results from a single spot measurement of 20 to 70 µm droplets (see fig. 3)? A discussion about the legitimacy of Raman micro-spectroscopy for immersion mode measurements is absolutely necessary. For a reader, the experimental work appears in that way, that only the optical part of the microscope was used for obtaining the dataset, but not the Raman spectrometer.***

The authors thank the referee for making the valid point that we do not show any Raman spectra for the immersion freezing experiments. Unfortunately, this is because Raman spectroscopy was not utilized during immersion freezing experiments. This was largely because Raman spectra of water droplets containing volcanic ash or minerals were dominated by the -OH stretch due to liquid water. The authors agree that including the phrase "using Raman Spectroscopy" in the title may be misleading. Thus, the authors have removed the phrase "using Raman Spectroscopy" from the title.

) The authors claim that up to now only two datasets have been used to suggest one characteristic ice nucleation efficiency. They extended the dataset from two to five ash samples. There is no statistical confidence within this interpretation. How can the authors reliable conclude that immersion mode freezing is dependent on the composition of the ash by this limited dataset?

The authors agree that the immersion freezing of volcanic ash may not be entirely dependent on the composition of the ash. Thus, the following sentence has been added Page 1401, line 8:

"It is important to note that the above discussion interprets immersion freezing only from a chemical mechanism standpoint."

) How was sampling of the volcanic ashes done? Were the samples collected from the nearby ash fall around the volcanos? How long were the ashes exposed to environmental conditions after the eruptions of the related volcanos? Are particles which settle close to the volcano comparable with fly-ash which is able to cover a distance of several hundreds of kilometres? Is there a general independence of the chemical composition, environmental aging from the size and the difference in exposure (atmosphere, soil, . . .)?

The authors agree that the volcanic ash sampling details were not sufficiently detailed. Thus, the paragraph start on page 1389, line 11 now reads:

"Volcanic ash was collected from three separate volcanic eruptions that produced three distinct types of ash. Volcan Fuego (14.4828° N, 90.8828° W) is an active stratovolcano that lies 16 km north of Antigua, Guatemala. The sub-Plinian eruption of October 14, 1974 produced ash fall that impacted an area of ~400 km^2, and samples used here were collected by previous researchers immediately after eruption from a location 10 km from the vent. The Soufrière Hills volcano (16.7167° N, 62.1833° W) is an active stratovolcano located in Montserrat, an island in the Lesser Antilles island arc of the West Indies. The ongoing eruption, which began in 1995, produces cyclic dome-building and explosive activity, with samples used here resulting from an explosion in January of 2010; samples were collected immediately after deposition < 3 km from the vent. Finally, the Taupo caldera (38.8056° S, 175.9008° E) sits in the center of the North Island of New Zealand. Samples used here were collected from air fall deposits of the Oruanui ultra-Plinian eruption ~26 ka. The samples were excavated 39 km from the vent 25.4 ka after the eruption."

The authors also acknowledge that there may not be a general independence of chemical composition and due to distances from the vent or environmental aging; unfortunately, such questions probe complex chemical mechanisms that are beyond the scope of this work. To highlight this we have added the following sentence to Page 1390, line 7:

"Chemical differences due to collection distances from the vent or environmental aging were not explicitly taken into account in this study."

General minor issues:

) Raman spectra in figure 1 (and others): These Raman spectra are displayed like they were measured in the anti-Stokes mode. Are these anti-Stokes spectra or are the spectra displayed in

an unusual way for Stokes-Raman spectra. Further, assignment of the Raman excitations would improve the quality of the figure and assist a detailed understanding of the work.

While the authors agree that the Raman spectra are displayed as if they were measured in the anti-Stokes mode, we have traditionally presented the Raman spectra from our Raman microscope in this orientation. This decision was made to accommodate readers in the fields of atmospheric chemistry and physics who, the authors assume, are generally more familiar with infrared spectroscopy. To clarify this, we have altered Page 1391, line 5 to now read "Stokes-mode Raman spectra."

****) Sampling: Indication of the geo-coordinates of the volcanos and the sampling site as well as the distance from the sampling site to the craters would be helpful.***

See comments above about sampling.

Response to Zamin A. Kanji

The referee's comments are bolded and italicized while our comments are in plain text

This manuscript discusses the deposition and immersion mode ice nucleation behavior of three volcanic ash samples as well as Kaolinite (KGa-1b) and Na/Ca Feldspar as references. The data presented is of timely interest to the readers of ACP, in particular the ice nucleation community. The methods used are sound and have been validated before in previous publications. The major conclusion is that not all volcanic ash samples have the same ice nucleation activity in immersion mode. In addition, Na/Ca Feldspar content was not found to be a good predictor of ice nucleation efficiency, rather it is proposed that the Silica (quartz) content would better explain the ice nucleation ranking behaviour of the ash samples in immersion freezing. The paper is written well and limitations are also discussed. I have suggested a few minor revisions, additions and have a few questions, all indicated directly in the manuscript. I recommend the paper to be published after the minor comments are addressed.

The author's would first like to thank Dr. Kanji for his insightful comments that have improved the clarity of this manuscript

Specific Comments:

Page 1387, line 21: You could consider using INP, this is not necessary but something to consider in case you have not

While this is a valid suggestion that is prevalent in the ice nucleation literation, the authors prefer to use ice nuclei (IN) to ice-nucleating particles (INP) in order to differentiate between heterogeneous ice nuclei and particles that freeze homogeneously, as well as avoid confusion with the also-common "ice nucleation protein."

Page 1388, line 18: What type of classification, minerology or emission mass, content?

The authors agree that the phrase "similar classifications" is vague and perhaps inappropriate to use when comparing only two samples. Thus the text has been changed on Page 1388, line 18 to read "these results represent only two volcanoes."

Page 1388, line 23: Maybe some more information on what this means, for the readership of the paper. It may be obvious to geologists/volcanologists but maybe not to cloud microphysicists and atmospheric scientist.

The authors agree that this terminology may be unfamiliar to cloud microphysicists and atmospheric scientist who are the target audience for this paper. Thus, Page 1388, line 23 has now been changed to read "which are basaltic (45-52% SiO_2), andesitic (56-59% SiO_2), and rhyolitic ashes (63-75% SiO_2) (Heiken, 1972), respectively."

Page 1389, line 1: Would be nice to specify the type of Ka here. We know different batches have different IN activity in particular the samples from CMS are different from Fluka.

Given this papers focus on linking mineralogy to ice nucleation efficiency, the authors agree that the type of kaolinite should be specified here. Thus, Page 1389, line 1 now readers "kaolinite (KGa-1b, Sihvonen et al, 2014)."

Page 1389, lines 15-21: When was the sample conducted relative to the eruption? Date of samping?

The authors agree that both the location and sampling date provide important insights into the results of the study. Thus, the paragraph start on page 1389, line 11 now reads:

"Volcanic ash was collected from three separate volcanic eruptions that produced three distinct types of ash. Volcan Fuego (14.4828° N, 90.8828° W) is an active stratovolcano that lies 16 km north of Antigua, Guatemala. The sub-Plinian eruption of October 14, 1974 produced ash fall that impacted an area of ~400 km^2, and samples used here were collected by previous researchers immediately after eruption from a location 10 km from the vent. The Soufrière Hills volcano (16.7167° N, 62.1833° W) is an active stratovolcano located in Montserrat, an island in the Lesser Antilles island arc of the West Indies. The ongoing eruption, which began in 1995, produces cyclic dome-building and explosive activity, with samples used here resulting from an explosion in January of 2010; samples were collected immediately after deposition < 3 km from the vent. Finally, the Taupo caldera (38.8056° S, 175.9008° E) sits in the center of the North Island of New Zealand. Samples used here were collected from air fall deposits of the Oruanui ultra-Plinian eruption ~26 ka. The samples were excavated 39 km from the vent 25.4 ka after the eruption."

Page 1392, line 10: Were there conditions at which ice formed on the fused-silica disc? If so, what were the temp and RH conditions when you observed this? And could this have occurred else where on the stage not under the field of view of the microscope

The authors agree that ice formation on the substrate could provide a significant artifact in the experiment and reporting the conditions at which this occurs is important. These results have been previously reported in Baustian et al., 2010. Thus the following line was added to Page 1392, line 10:

"We have previously reported the conditions under which a blank fused-silica disc initiates ice formation (Baustian et al., 2010). In that study, we found that the blank substrate nucleated ice at S_{ice} of 1.6 to 2.33 from ~235 to 215 K."

Page 1393, line 26: Can you distinguish if the ice formed before the contact or the contact occurred before the ice nucleation? See comment at Figure 3.

The authors agree that care should be taken our immersion freezing analysis not to include contact freezing events. Such precautions were taken, and the text starting on Page 1393, line 26 has now been revised to read:

"Further, by recording 30 frame-per-second video, we could unambiguously determine if droplets coagulated or froze by contact freezing. In all experiments, no contact-freezing events occurred from the contact of two liquid drops. If two droplets coagulated, their coagulated droplet size was

considered. Unfrozen droplets, however, could be frozen by contact with growing ice particles; those contact-frozen droplets were disregarded in our analysis."

Page 1394, line 21: What are the silica contents different in Table 1 and 2?

The authors acknowledge that the difference between silica content and quartz content was not sufficiently explained in the discussion paper. The silica content of the ash is determined from elemental analyses, most commonly as X-ray fluorescence, and will include Si contributions from the melt glass, minerals, and lithic materials in the ash. Quartz is a pure, crystalline form of SiO_2, and its content is determined from X-ray diffraction. To clarify this in the text, we have added the following sentences to Page 1390, line 1:

"It is important to note that silica content of the ash is determined from elemental analyses, most commonly as X-ray fluorescence, and will include Si contributions from the melt glass, minerals, and lithic materials in the ash; this is not to be confused with quartz, which can be one mineral component of the ash composed is pure, crystalline SiO_2."

Page 1398, line 5: Why not calculate nucleation rates if you really would like to take time dependence into account? And compare nucleation rates to one another?

While the authors agree that calculating nucleation rates and comparing those nucleation rates to previous studies would indeed be taking time dependence into account, the focus of this exercise was to validate our immersion freezing setups with a material and framework (i.e., the singular approximation) used by both continuous flow and cold stage instruments. Finally, while an in-depth discussion of the time-dependence of heterogeneous ice nucleation would be an interesting area to explore, to fully analyze it is beyond the capabilities of this data set.

Page 1411: Why is the silica content here different from that in Table 1?

See comments above about silica content.

Page 1412: There is an appearance of a small peak in the ground and nebulized sample. What is this attributed to and shouldn't it be addressed.

The authors agree that there is a small peak near 663 cm^{-1} that is present in the ground and the ground/nebulized samples, but not present in the unground samples. Since volcanic ash is a complex mixture of volcanic glass, minerals, and possibly lithic material, peak identification is outside of the scope of this manuscript. We do, however, postulate that this peak emerges due to better homogeneity of the ground samples. To highlight this, another vertical dashed line has been added to Figure 1 and the following passages have been altered in the manuscript to read:

Page 1391, line 20: "An example set of these spectra for Soufrière Hills ash is shown in Fig. 1. It can be seen that the main ash signatures at 507 cm^{-1}, 408 cm^{-1}, and 281 cm^{-1} in the Raman spectra are not significantly altered between the unground, ground, and aggregated particles, indicating that any major chemical alteration due to ash processing was not detected for these samples. A small peak at 663 cm^{-1}, however, does appear in the ground and ground/nebulized and dried ash; we attribute this peak this better homogeneity of minor components within the ground samples as compared to the unground samples."

Page 1412: "A set of example Raman spectra of unground, ground, and ground/nebulized Soufrière Hills volcanic ash. As shown, the main peaks at 507 cm^{-1}, 408 cm^{-1}, and 281 cm^{-1} (vertical dashed lines) are minimally affected by mechanical grinding and wet generation, suggesting that bulk chemical alteration does not occur. A small peak at 663 cm^{-1}, however, does appear in the ground samples, possibly due to better homogeneity of minor components when compared to unground samples."

Page 1414: Is it possible to provide a more magnified version of this figure, where the lack of structure ans appearance of a structure in the frozen droplets is more evident. It is not super clear in these figures. Although if one observed closely, the bottom figure does have a few crystals with protrusions that would imply ice formation.

Unfortunately, video recordings of the experiments were taken at 20x magnification in order to view a statistically significant number of particles within the image frame. Magnifying the images would not increase the level of detail within the image.

Page 1414: If the droplets continue to coagulate even after you have stopped depositing the particles on the stage and during the cooling process, this needs to be made clear. It is also evident from the images that in the liquid phase there are more droplets than in the image where ice is present. So is this only due to the bergeron-findeisen process or could it be from contact nucleation with the small droplets diffusing to the large ones as pointed out in the image.

See comments above about droplet coagulation and contact freezing.

Page 1415: Kelvin here, but degrees C in the next plot, then you switch back to Kelvin. Why? Can you just chose one and stick to it?

The authors agree that switching between the two temperature scales is confusing; however to better compare figures to previous work in the literature, we have kept all frozen fraction curves in the Celsius scale and all n_s and S_{ice} plots in the Kelvin scale.

Page 1419: Are these data points that cover homogeneous nucleation, if so, you may consider removing them from this plot. To me it looks like these drops based on plots from Figure 7, froze homogeneously, then I think that there is no need to plot them on an ns curve, since the surface area should not matter for hteir freezing. This is also implicit by the steep slope. You may want to comment about the lack of temperature dependence or the different temperature dependence here for these data point.

The authors agree that the points below ~238 K may be due to homogeneous freezing as indicated by their steep slope in Figure 8 and their coincidence with the homogeneous freezing curve in Figure 7. Thus, the temperature range on Figure 8 has been altered to truncate at 238 K.

Minor Changes

The word "for" has been added to Page 1387, line 4.

"Further" has been changed to "furthermore" on Page 1387, line 11.

The word "ice" has been deleted Page 1387, line 13.

The reference Hoyle et al., 2011 ACP has been added to Page 1388, line 4.

The phrase “in modifying the composition of the aerosolized ash” has been added to Page 1389, line 24.

The phrase “droplet size” has been added to Page 1393, line 22, so that it now reads “and 65-165 µm (droplets size, lateral diameter).”

The last sentence on Page 1393 has been changed for clarity. It now reads “The temperature error of 0.5 K for all droplets was determined by repeated homogeneous freezing experiments of ultra-pure water.”

The phrase “in the temperature range investigated” has been added to Page 1395, line 9.

The “Hiranuma et al., 2014a” reference on Page 1398, line 14 has been changed to “Hiranuma et al., 2015.” This has also been changed in the reference section.

Response #2 to Zamin A. Kanji

The referee's comments are bolded and italicized while our comments are in plain text.

Major Comments

Page 10, line 213: "Can you address this choice of cooling rate, this seems high."

The authors agree that providing a reason for this cooling rate would enhance the description of our experimental setup. As mentioned on Page 11, Line 218, in some cases mass transfer from supercooled droplets to frozen droplets can cause liquid droplets to shrink and disappear or be frozen by contact by a growing ice crystal; to minimize these effects, a high cooling rate is desired. Cooling rates that are too high, however, will lead to an offset between the measured temperature and the actual temperature because of heat transfer limitations between the cold-stage and fused-silica disc. Thus, we chose a cooling rate of 10 K min^{-1}, which minimizes the aforementioned mass-transfer effects without causing a measureable offset between the measured and actual temperatures. This optimal cooling rate has been determined for cold stages in previous publications (e.g., Koop et al., 1998). To express this, we have added the following text to Page 11, Line 225:

"To minimize liquid droplet shrinking and contact-freezing by growing ice crystals, we have chosen a cooling rate of 10 K min^{-1}. This rate strikes a balance of minimizing the aforementioned mass-transfer effects while avoiding a measurable temperature offset between the measured and actual temperature of the particles on the fused-silica disc due to heat-transfer limitations that occur at higher cooling rates. (Koop et al., 1998)."

And the following reference to the "References" section:

"Koop, T., Ng, H. P., Molina, L. T., and Molina, M. J.: A new optical technique to study aerosol phase transitions: The nucleation of ice from H2SO4 aerosols, J. Phys. Chem. A, 102, 8924-8931, doi:10.1021/jp9828078, 1998."

Page 34, line 540: The scale is decreasing in the wrong direction. Cartesian co-ordinates require the scale to increase going from left to right.

Dr. Kanji makes an excellent point that the scale is decreasing in wrong direction. We have altered Figure 8 to read correctly in Cartesian coordinates.

Page 34, line 540: "I am not sure I understand or agree with the reasoning behind leaving this axis in K. The authors already plot previous data from the literature in this plot. Not sure why changing the acis to Celsius would take away from the ability to compare to previous work.

The authors now agree that there is no reason why all immersion freezing figures cannot be displayed in one temperature scale. Thus, Figures 6 and 8 are now shown in the Celsius scale instead of in the Kelvin scale.

Page 34, line 540: "The units don't match the scale"

The authors thank Dr. Kanji for finding this error. The x-axis on Figure 8 is now reported in Celsius.

Minor Comments

Page 9, Line 168: The word "to" has been added so now that line reads "we attribute this peak to better homogeneity …"

Page 16, Line 333: The 4 in 2014 was deleted in the final markup

Page 22, Line 480: A degree sign was added after -15 and before C

Page 28, Line 516: The scale label was placed directly on Figure 3 and the text in Figure 3 that read "The scale bar in the bottom-right hand corner equals 100 μm." The same was done for Figure 2.

Relevant Changes (Response to Referees)

Page 1, line 2: Deleted "using Raman Spectroscopy" from the title

Page 3, line 38: Added "for"

Page 3, line 46: "Further" now reads "furthermore"

Page 3, line 47: Deleted "ice"

Page 4, line 64: Added the reference "Hoyle et al., 2011"

Page 5, line 76: This sentence has been altered for clarity. It now reads "these results represent only two volcanoes."

Page 5, line 81: This sentence has been altered for clarity. It now reads "which are basaltic (45-52% SiO_2), andesitic (56-59% SiO_2), and rhyolitic ashes (63-75% SiO_2) (Heiken, 1972), respectively.

Page 5, line 88: The type of clay, "KGa-1b," has been specified.

Page 5, line 97: The paragraph starting here has been altered to provide a more detailed description of the ash sampling. It now reads

> "Volcanic ash was collected from three separate volcanic eruptions that produced three distinct types of ash. Volcan Fuego (14.4828° N, 90.8828° W) is an active stratovolcano that lies 16 km north of Antigua, Guatemala. The sub-Plinian eruption of October 14, 1974 produced ash fall that impacted an area of ~400 km^2, and samples used here were collected by previous researchers immediately after eruption from a location 10 km from the vent. The Soufrière Hills volcano (16.7167° N, 62.1833° W) is an active stratovolcano located in Montserrat, an island in the Lesser Antilles island arc of the West Indies. The ongoing eruption, which began in 1995, produces cyclic dome-building and explosive activity, with samples used here resulting from an explosion in January of 2010; samples were collected immediately after deposition < 3 km from the vent. Finally, the Taupo caldera (38.8056° S, 175.9008° E) sits in the center of the North Island of New Zealand. Samples used here were collected from air fall deposits of the Oruanui ultra-Plinian eruption ~26 ka. The samples were excavated 39 km from the vent 25.4 ka after the eruption."

Page 6, line 111: Added the phrase "in modifying the composition of the aerosolized ash."

Page 6 line 114: Added the sentence "It is important to note that silica content of the ash is determined from elemental analyses, most commonly as X-ray fluorescence, and will include Si contributions from the melt glass, minerals, and lithic materials in the ash; this is not to be confused with quartz, which can be one mineral component of the ash composed is pure, crystalline SiO_2."

Page 7, line 123: Added the sentence "Chemical differences due to collection distances from the vent or environmental aging were not explicitly taken into account in this study."

Page 8, line 148: Added "Stokes-mode" to clarify the type of Raman spectra display

Page 8, line 164: The following sentences have been altered to account for a small peak at 663 cm^{-1} appearing in the ground spectra. It now reads

> "It can be seen that the main ash signatures at 507 cm^{-1}, 408 cm^{-1}, and 281 cm^{-1} in the Raman spectra are not significantly altered between the unground, ground, and aggregated particles, indicating that any major chemical alteration due to ash processing was not detected for these samples. A small peak at 663 cm^{-1}, however, does appear in the ground and ground/nebulized and dried ash; we attribute this peak this better homogeneity of minor components within the ground samples as compared to the unground samples."

Page 9, line 168: The word "to" has been added so now that line reads "we attribute this peak to better homogeneity …"

Page 9, line 180: Added the following sentence: "We have previously reported the conditions under which a blank fused-silica initiates ice formation (Baustian et al., 2010). In that study, we found that the blank substrate nucleated ice at S_{ice} of 1.6 to 2.33 from ~235 to 215 K."

Page 11, line 217: Added "droplet size"

Page 11, line 220: The following sentences were altered to clarify that, in our experiments, we can distinguish between immersion and contact freezing. These sentences now reads

> "Further, by recording 30 frame-per-second video, we could unambiguously determine if droplets coagulated or froze by contact freezing. In all experiments, no contact-freezing events occurred from the contact of two liquid drops. If two droplets coagulated, only their coagulated droplet size was considered. Unfrozen droplets, however, could be frozen by contact with growing ice particles; those contact-frozen droplets were disregarded in our analysis. Errors in n_s values are based on the range of surface areas available in each experiment. The temperature error of 0.5 K for all droplets was determined by repeated homogeneous freezing experiments of ultra-pure water."

Page 11, line 220: The following sentences were added to clarify our choice of cooling rate in our immersion freezing experiments:

> "To minimize liquid droplet shrinking and contact-freezing by growing ice crystals, we have chosen a cooling rate of 10 K min^{-1}. This rate strikes a balance of minimizing the aforementioned mass-transfer effects while avoiding a measurable temperature offset between the measured and actual temperature of the particles on the fused-silica disc due to heat-transfer limitations that occur at higher cooling rates. (Koop et al., 1998)."

Page 12, line 256: The phrase "in the temperature range investigated" was added.

Page 16, line 333: Hiranuma et al., 2014b has been changed to Hiranuma et al., 2015

Page 17, line 362: Hiranuma et al., 2014b has been changed to Hiranuma et al., 2015

Page 19, line 403: Added the sentence "It is important to note that the above discussion interprets immersion freezing only from a chemical mechanism standpoint."

Page 22, line 480: A degree sign was added after -15 and before C

Page 26, line 501: Figure 1 was altered to contain an additional vertical dashed line at 663 cm^{-1}

Page 26, line 505: Added the following sentence to the caption of Figure 1: "A small peak at 663 cm^{-1}, however, does appear in the ground samples, possibly due to better homogeneity of minor components when compared to unground samples."

Page 27, line 512: The scale label was placed directly on Figure 2 and the text in Figure 2 that read "The scale bar in the bottom-right hand corner equals 10 μm."

Page 28, line 516: The scale label was placed directly on Figure 3 and the text in Figure 3 that read "The scale bar in the bottom-right hand corner equals 100 μm."

Page 31, line 534: Figure 6 was altered such that the X

Page 34, line 540: Figure 8 was altered such that the X-axis was changed from the Kelvin scale to the Celsius scale, the x-axis was altered so that it is increasing from left to right, and the (new) left-hand side of the x-axis ends at -35 °C.

Page 37, line 596: Altered the Hiranuma et al., 2014b ACPD reference to be the Hiranuma et al., 2015 ACP reference.

Page 38, line 639: Added the reference to Koop et al., 1998.

Relevant Changes (Authors Decision):

Page 10, line 203: The blank substrate was erroneously labeled "quartz." It has now been changed to "fused silica."

Page 18, line 394: In light of recent work published by Zolles et al., (2015), the following line was deleted: "To our knowledge, a laboratory standard of Na/Ca-feldspar cannot be obtained without these K-feldspar impurities."

Page 18, line 397: In light of recent work published by Zolles et al., (2015), the following line was added: "This is in agreement with Zolles et al. (2015), who found that the Na/Ca-feldspars albite and anorthian andesine as well as an albite-dominated ash sample were all weak immersion-mode IN."

Page 22, line 477: In the discussion manuscript, the authors had missed an important reference by Seifert et al., 2011. In light of this, we have added

> "Furthermore, a study using polarization lidars at two central-European stations found a clear influence of volcanic ash on heterogeneous ice nucleation of tropospheric clouds. For example, in that study, all observed cloud layers with cloud top temperatures < -15 C contained ice during the days following the April 2010 Eyjafjallajökull volcanic eruption (Seifert et al., 2011)."

Page 40, line 684: Added the Seifert et al., 2011 reference to the reference section.

Page 41, line 725: Added the Zolles et al., 2015 reference to the reference section.

Deposition and Immersion Mode Nucleation of Ice by Three Distinct Samples of Volcanic Ash ~~Using Raman Spectroscopy~~

Gregory P. Schill[1,*], Kimberly Genareau[2], and Margaret A. Tolbert[1]

[1]{Department of Chemistry and Biochemistry and Cooperative Institute for Research in Environmental Science, University of Colorado, Boulder, CO, USA}

[2]{Department of Geological Sciences, University of Alabama, Tuscaloosa, AL, USA}

[*]{Now at Department of Atmospheric Sciences, Colorado State University, Fort Collins, CO, USA}

Correspondence to: M.A. Tolbert (tolbert@colorado.edu)

Abstract

Ice nucleation on volcanic ash controls both ash aggregation and cloud glaciation, which affect atmospheric transport and global climate. Previously, it has been suggested that there is one characteristic ice nucleation efficiency for all volcanic ash, regardless of its composition, when accounting for surface area; however, this claim is derived from data from only two volcanic eruptions. In this work, we have studied the depositional and immersion freezing efficiency of three distinct samples of volcanic ash using Raman Microscopy coupled to an environmental cell. Ash from the Fuego (basaltic ash, Guatemala), Soufrière Hills (andesitic ash, Montserrat), and Taupo (Oruanui euption, rhyolitic ash, New Zealand) volcanoes were chosen to represent different geographical locations and silica content. All ash samples were quantitatively analyzed for both percent crystallinity and mineralogy using X-ray diffraction. In the present study, we find that all three samples of volcanic ash are excellent depositional ice nuclei, nucleating ice from 225-235 K

at ice saturation ratios of 1.05 ± 0.01, comparable to the mineral dust proxy kaolinite. Since depositional ice nucleation will be more important at colder temperatures, fine volcanic ash may represent a global source of cold-cloud ice nuclei. For immersion freezing relevant to mixed-phase clouds, however, only the Oruanui ash exhibited heterogeneous ice nucleation activity. Similar to recent studies on mineral dust, we suggest that the mineralogy of volcanic ash may dictate its ice nucleation activity in the immersion mode.

1 INTRODUCTION

It is estimated that approximately 9% of the world's population lives within 100 km of a historically active volcano (Small and Naumann, 2001) and at any moment at least 20 volcanoes around the globe may be erupting (Durant et al., 2010). In these areas, both gaseous and particulate volcanic emissions can affect both human respiratory health (Horwell and Baxter, 2006) and local environments (Witham et al., 2005). Further, explosive volcanic eruptions can greatly influence global climate, even for years after the initial eruption (Durant et al., 2010). For example, the eruption of Mt. Pinatubo in 1991 injected large amounts of gaseous sulfur species into the stratosphere, which perturbed the climate system for 2-3 years following the eruption (Robock, 2004).

In addition to gaseous emissions, explosive volcanoes generate large amounts of fine ash (< 63 μm), which is dispersed into the atmosphere via plumes above volcanic vents and pyroclastic flows. The global annual flux of fine volcanic ash into the atmosphere is approximately 200 Tg yr^{-1}, based on a 1000-yr average. While this flux is smaller than the terrestrial dust burden of approximately 1000 to 4000 Tg yr^{-1} (Huneeus et al., 2011), volcanic eruptions are often sporadic and can eject a large amount of particulate into the atmosphere over a short amount of time. Furthermore, water vapor is abundant in volcanic eruptions, with up to 8% of the pre-eruptive magma by mass (Durant et al., 2008). Thus, volcanic plumes represent prime conditions for ~~ice~~ cloud glaciation via heterogeneous ice nucleation, yet this phenomenon is vastly understudied considering its influence on plume dynamics, volcanic lightning, sequestration of gaseous species, and the transport of these species to the stratosphere (Brown et al., 2012;McNutt and Williams, 2010;Kolb et al., 2010;Van Eaton et al., 2012). Further, fine ash from plumes can stay suspended in the upper troposphere for weeks to months and travel 1000s of kilometers; if these particles are

efficient depositional ice nuclei, they could represent a widespread source of cold-cloud ice nuclei not currently parameterized in global models (Hoose et al., 2010).

Active volcanoes have long been known to influence ice nuclei (IN) concentrations in the atmosphere (Hobbs et al., 1971;Isono et al., 1959). For example, a study monitoring IN concentrations in Japan found concentrations were enhanced by a factor of 40 over background aerosol following the eruption of a nearby active volcano (Isono et al., 1959). In contrast, other studies have shown that IN concentrations near volcanic plumes were not elevated above typical background concentrations (Langer et al., 1974;Schnell and Delany, 1976). It was suggested, however, that the ash in some of these studies had been deactivated by chemical processing via gases in the volcanic cloud.

Laboratory studies probing the ice nucleation efficiency of volcanic ash have also shown it can act as a heterogeneous IN (Durant et al., 2008;Hoyle et al., 2011). Unlike field measurements, however, it has been suggested that all volcanic ash may have similar ice nucleation efficacy, initiating ice formation in a relatively narrow temperature range of approximately 250 to 260 K (Durant et al., 2008); however, these works are difficult to interpret quantitatively, especially in cases where the nucleation mode is unclear, frozen fractions are unavailable, or the available surface area has not been quantified. More recently, several studies have investigated the deposition and/or immersion mode ice nucleation properties of ash from the 2010 eruption of the Eyjafjallajökull volcano in Iceland (Steinke et al., 2011;Hoyle et al., 2011;Bingemer et al., 2012). The results of these studies, combined with previous studies on large, 250-300 μm ash particles from the 1980 Mt. St. Helens eruption (Fornea et al., 2009), suggests that there is one characteristic ice nucleation efficiency for all ash, even when accounting for frozen fractions and surface area (Murray et al., 2012). While such behavior would allow for a great simplification in models, these

results represent~~are~~ only ~~for~~ two volcanoes~~. with similar classifications~~. Thus, the question still remains of whether or not all volcanic ash exhibits similar ice nucleation activity regardless of the location, pre-eruptive magma composition, and mineralogy.

In this study, we have collected volcanic ash particles from the Fuego (Guatemala), Soufrière Hills (Montserrat), and Taupo (Oruanui eruption, New Zealand) volcanoes, which are basaltic (45-52% SiO_2), andesitic (56-59% SiO_2), and rhyolitic ashes (63-75% SiO_2) (Heiken, 1972), respectively. These samples were specifically chosen to represent three separate geographical locations, classifications by silica content, and percent minerals. For each of these ashes, we have probed their depositional ice nucleation and immersion freezing potential. The present experiment used to study depositional ice nucleation has been described previously; however, this paper represents our first measurements of immersion freezing. For the depositional nucleation experiments, the results are compared to previous results using the same system for the clay mineral kaolinite (KGa-1b, Sihvonen et al., 2014), which is generally thought to be an efficient depositional IN (Hoose and Moehler, 2012). For the immersion freezing experiments, the Raman Microscope cold stage was validated using the same, standard kaolinite sample (Murray et al., 2011;Pinti et al., 2012). Using this validated system, we determined the ice nucleation active surface site densities of each volcanic ash sample by utilizing the singular description (Vali, 1994, 2008;Vali and Stansbury, 1966). The results and implications of these findings for cloud glaciation in volcanic plumes and the atmosphere are discussed.

2 EXPERIMENTAL

2.1 Volcanic Ash and Standard Minerals

Volcanic ash was collected from three separate volcanic eruptions that produced three distinct types of ash. Volcan Fuego (14.4828° N, 90.8828° W) is an active stratovolcano that lies 16 km

north of Antigua, Guatemala. The sub-Plinian eruption of October 14, 1974 produced ash fall that impacted an area of ~400 km^2, and samples used here were collected by previous researchers immediately after eruption from a location 10 km from the vent. The Soufrière Hills volcano (16.7167° N, 62.1833° W) is an active stratovolcano located in Montserrat, an island in the Lesser Antilles island arc of the West Indies. The ongoing eruption, which began in 1995, produces cyclic dome-building and explosive activity, with samples used here resulting from an explosion in January of 2010; samples were collected immediately after deposition < 3 km from the vent. Finally, the Taupo caldera (38.8056° S, 175.9008° E) sits in the center of the North Island of New Zealand. Samples used here were collected from air fall deposits of the Oruanui ultra-Plinian eruption ~26 ka. The samples were excavated 39 km from the vent 25.4 ka after the eruption.

Volcanic ash (pyroclasts < 2 mm) dominantly consists of silica-rich volcanic glass and crystalline minerals. The chemical composition of volcanic ash is mainly determined from its parent magma, although lithic material from the vent may play a role in modifying the composition of the aerosolized ash. Since the main chemical elements of magma are Si and O, magma is often classified by its silica content, which increases in the following order: basaltic (45-52% SiO_2), andesitic (56-59% SiO_2), and rhyolitic (63-75% SiO_2) (Heiken, 1972). It is important to note that silica content of the ash is determined from elemental analyses, most commonly as X-ray fluorescence, and will include Si contributions from the melt glass, minerals, and lithic materials in the ash; this is not to be confused with quartz, which can be one mineral component of the ash composed is pure, crystalline SiO_2. Each parent magma has a different melting temperature, viscosity, and volatile content (dominantly H_2O); further, the assemblage and composition of minerals often reflect their host melt (Langmann, 2014). The silica content and % crystals, taken from previous whole-rock studies, for each of the volcanoes are shown in Table 1. As shown, the

Fuego, Soufrière Hills, and Oruanui whole-rock samples represent a range of magma compositions and contain varying amounts of crystalline material. Chemical differences due to collection distances from the vent or environmental aging were not explicitly taken into account in this study. From these bulk studies, the primary mineral for all three samples was found to be plagioclase, a tetrosilicate material in the feldspar family; however the samples vary in their next abundant mineral. For the Fuego, Soufrière Hills, and Oruanui samples, the second-most abundant mineral is olivine, amphibole, and quartz, respectively.

A low-defect kaolinite from Washington County, GA, USA (KGa-1b) was obtained from the Source Clays Repository of the Clay Mineral Society (West Lafayette, IN, USA). KGa-1b was chosen because it has been previously been studied in the ice nucleation literature in both the deposition and immersion mode (Hoose and Moehler, 2012; Murray et al., 2012). Soda feldspar [Standard Reference Material (SRM) 99b], a standard Na/Ca-feldspar, was obtained from the National Institute of Standards and Technology (NIST) as a homogenous, fine powder (< 60 µm).

2.2 Raman Microscope and Environmental Cell

The Raman microscope has been described previously in detail (Baustian et al., 2010;Schill and Tolbert, 2013). Briefly, a Nicolet Almega XR Raman spectrometer has been coupled to a research grade Olympus BX-51 microscope with 10x, 20x, 50x, and 100x magnification objectives. This Raman microscope has been outfitted with a Linkam THMS600 environmental cell. The temperature of a cold stage inside the cell is controlled by a Linkam TMS94 automated temperature controller with an accuracy of 0.1 K. Water partial pressure inside the cell is controlled by mixing dry and humidified flows of N_2 and measured using a Buck Research CR-A1 dew point hygrometer in line with the cell. The accuracy of the dew point hygrometer is 0.15 K. The relative humidity (RH) and ice saturation ratio ($S_{ice} = P_{H2O}/VP_{ice}$) inside the cell are determined by ratioing

the partial pressure of water to the equilibrium vapor pressure of water and ice, respectively (Murphy and Koop, 2005). A Gast diaphragm pump at the exit of the hygrometer ensures that the gas flow through the cell and hygrometer is 1 L min^{-1}.

Stokes-mode Raman spectra were obtained using a 532 nm frequency-doubled Nd:YAG as the excitation laser. Spectra were taken from 200 to 4000 cm^{-1} with a typical resolution of 2-4 cm^{-1}. Spectra were taken at the center of each particle and typically consisted of 256 co-added scans and were taken with 50x and 100x long-range objectives, which focus the laser to a spot size of approximately 1.3 and 1.1 µm, respectively (Everall, 2010). .

2.3 Depositional Freezing

For depositional freezing experiments, approximately 100 mg of ash was ground in a porcelain mortar and pestle. To the ground ash, 8.0 mL of ultra-pure water was added and the slurry was immediately aspirated into a Meinhard TR-50 glass concentric nebulizer. Nebulized droplets were directed at a fused-silica disc and allowed to coagulate into supermicron droplets. The sample disc was then transferred into the environmental cell and exposed to a low humidity environment. This caused water evaporation, resulting in aggregated ash particles ranging from 1 to 20 µm in lateral diameter. Similar composite or aggregate volcanic ash samples are often found in the atmosphere, and are produced by a similar mechanism (Brown et al., 2012). To assure that minimal chemical alteration occurred from grinding and nebulizing the ash samples, Raman spectra of unground, ground, and ground/nebulized and dried ash were obtained. An example set of these spectra for Soufrière Hills ash is shown in Fig. 1. It can be seen that the main ash signatures at 507 cm^{-1}, 408 cm^{-1}, and 281 cm^{-1} in the Raman spectra are not significantly altered between the unground, ground, and aggregated particles, indicating that any major chemical alteration due to ash processing was not detected for these samples. A small peak at 663 cm^{-1}, however, does appear in

the ground and ground/nebulized and dried ash; we attribute this peak to better homogeneity of minor components within the ground samples as compared to the unground samples.

Depositional nucleation experiments were conducted from 225-235 K. Experiments consisted of increasing ice supersaturation over the sample by holding a constant vapor pressure of water and lowering the temperature until the first ice event was noted. Specifically, after the particles were allowed to sit at 298 K and ~0% RH for at least 10 minutes, the temperature was decreased at a rate of 10 K min^{-1}, until S_{ice} ~ 0.9. The temperature was then decreased at a rate of 0.1 K min^{-1}, which corresponds to an S_{ice} ramp rate of 0.01 min^{-1}, until the first ice event was noted. Initial observation of ice was monitored by scanning the entire disc using the 10x objective. After the first ice particle was detected, the 50x objective was utilized to verify the existence of ice both visually (Fig. 2a) and spectrally. Finally, the ice was sublimed by turning off the flow of the humidified nitrogen to ensure that ice had formed on an ash particle instead of the fused silica disc (Fig. 2b). We have previously reported the conditions under which a blank fused-silica disc initiates ice formation (Baustian et al., 2010). In that study, we found that the blank substrate nucleated ice at S_{ice} of 1.6 to 2.33 from ~235 to 215 K.

2.4 Immersion Freezing Experiments

For immersion freezing experiments, it was important to ensure that the concentration of volcanic ash or standard mineral in each drop was the same. Grinding with a mortar and pestle produced samples too coarse to meet these requirements. Thus, for immersion freezing experiments, a Wig-L-Bug® amalgamator (Crescent/Rinn Dental Mfg.) was used to pulverize volcanic ash or standard minerals (Hudson et al., 2008;Curtis et al., 2008). Specifically, approximately 100 mg of material was placed in a hardened stainless steel vial containing a stainless steel ball pestle. The samples were pulverized in four five-minute intervals, for a total of

twenty minutes. The samples were allowed to rest for five-minutes between intervals to avoid overheating of the sample. After treatment with the Wig-L-Bug®, the samples were made into 0.5, 1.0, and/or 2.0 wt% solutions with ultra-pure water. The concentration of material in suspensions was determined gravimetrically. Sample solutions were shaken for at least 12 h prior to ice nucleation experiments; this prevented unnecessary aggregation, and, therefore, ensured better homogeneity between droplets. To generate droplets for an immersion freezing experiment, a known weight-percent solution was aspirated into a Meinhard TR-30 glass concentric nebulizer. To mitigate gravimetric settling prior to nebulization, humidified nitrogen was vigorously bubbled through the sample solutions immediately before aspiration. Humidified N_2 was used as the carrier gas to prevent excess evaporation at the nebulizer nozzle (Todoli and Mermet, 2011). The nebulized spray was directed at a hydrophobically treated fused-silica disc, and the nebulized droplets were allowed to coagulate into supermicron droplets. After nebulization, the disc was immediately capped with an indium spacer (Alfa Aesar, 127 μm thick) and a second ~~quartz~~ fused-silica disc. The spacer was coated with Apiezon L high-vacuum grease to ensure good contact to the discs, which helped maintain a saturated humidity in the space created by the indium spacer (immersion cell). By taking the above precautions, the concentration of ash in each particle is assumed to be the same as the concentration of ash in the nebulized solution. To confirm this, droplets were examined under 50x magnification prior to each experiment to ensure that their ash concentrations were visually similar. Despite low relative humidities inside the environmental cell, droplets inside the immersion cell did not visibly grow or shrink, even after sitting for 12 h.

Freezing experiments were video recorded under 10x or 20x magnification at 30 frames per second, and freezing events were identified by the sudden appearance of structure within droplets. Droplets were cooled from approximately 5 °C to -40 °C at a rate of 10 K min^{-1}. An example of

droplets at the beginning of an immersion freezing experiment prior to freezing and the same droplets after all had frozen can be seen in Fig. 3a and 3b, respectively. Ice nucleation frozen fractions were calculated as a function of temperature. Frozen fraction curves were separated into two different size bins: 10-60 and 65-165 µm (droplet size, lateral diameter). These size bins span droplet volumes from ~1.3 pL to 0.7 nL. In some cases, larger ice particles would grow at the expense of smaller droplets in the cell. If these smaller droplets completely evaporated by the end of the experiment, they were disregarded in our analysis. Further, by recording 30 frame-per-second video, we could unambiguously determine if droplets coagulated or froze by contact freezing. In all experiments, no contact-freezing events occurred from the contact of two liquid drops. If two droplets coagulated, only their coagulated droplet size was considered. ~~if unfrozen~~ Unfrozen droplets, however, could be ~~were~~frozen by contact ~~frozen by~~with growing ice particles~~;~~, those contact-frozen droplets were ~~also~~ disregarded in our analysis. To minimize liquid droplet shrinking and contact-freezing by growing ice crystals, we have chosen a cooling rate of 10 K min^{-1}. This rate strikes a balance of minimizing the aforementioned mass-transfer effects while avoiding a measurable temperature offset between the measured and actual temperature of the particles on the fused-silica disc due to heat-transfer limitations that occur at higher cooling rates. (Koop et al., 1998). Errors in n_s values are based on the range of surface areas available in each experiment. The temperature error of 0.5 K for all droplets ~~, 0.5 K,~~ was determined by repeated homogeneous freezing experiments ~~on~~ of ultra-pure water.

2.5 Brunaur-Emmet-Teller Surface Areas

Brunaur-Emmet-Teller (BET) surface area analysis was conducted by Pacific Surface Sciences Inc. using a Micrometric TriStarr II surface area analyzer. For BET analysis, ash samples and Na/Ca-feldspar were prepared exactly as for immersion freezing experiments, but were not

suspended in high-purity water. The samples were degassed under flowing ultra-high purity grade nitrogen for two hours at a temperature of 200 °C and the surface area was measured. Nitrogen gas adsorption measurements were taken at relative pressures of 0.05, 0.1, 0.15, 0.2, and 0.25. The free space in the analysis tube was measured by the Helium method. The five pressure points were used to calculate the BET surface area. In this study, we determined the BET surface areas for all three volcanic ash samples and Na/Ca-feldspar (Table 1).

2.6 X-Ray Diffraction Analysis

X-Ray Diffraction (XRD) analysis of volcanic ash and Na/Ca-feldspar was conducted by X-Ray Wizards, LLC. Similar to BET analysis, each sample was prepared exactly as for immersion freezing, but was not suspended into solution. Data was collected with a Bruker D8 Discover instrument with a scintillation detector, Cu radiation, and appropriate slits for high resolution. Percent crystallinity and associated % amorphous were determined by profile fitting and Degree of Crystallinity measurements using the Bruker Rietveld Refinement (Table 1). Phase identification and quantitative analysis were used to determine the identity and relative amount of each phase in a mixture, and each identified mineral is reported as a wt% (Table 2). The quantitative analysis was done via reference intensity ratio.

3 RESULTS AND DISCUSSION

3.1 Depositional Ice Nucleation on Volcanic Ash Samples

Depositional ice nucleation experiments using the Raman microscope have previously been validated (Baustian et al., 2010;Wise et al., 2010). The critical S_{ice} needed for the onset of depositional ice nucleation on all three ash samples from 225-235 K is shown in Fig. 4. It can be seen that all three ash samples exhibit minimal temperature dependence and similar ice nucleation activity to each other at the temperatures explored. Further, all three ash samples require low ice

supersaturations (S_{ice} = 1.05 ± 0.01) to nucleate ice and, therefore, are efficient ice nuclei in the temperature range investigated. Also shown in Fig. 4 are onset results from depositional ice nucleation experiments on ash from the 2010 Eyjafjallajökull eruption from Hoyle et al. (2011) and Steinke et al. (2011). Here, even the Icelandic ash has similar ice nucleation activity to the three types of ash used in this study. To further highlight their depositional ice nucleation efficiency, a parameterization of the critical ice saturation ratio of kaolinite from a previous study (Sihvonen et al., 2014) has also been added to Fig. 4. Since these results were taken with the same instrument for similar frozen fractions and surface areas, these results are directly comparable. Thus, these results suggest it is possible that all volcanic ash studied to date are as efficient as clay minerals for ice nucleation in the depositional mode.

To attempt to elucidate why these ash samples had similar, efficient depositional ice nucleation abilities, we compared the % crystallinity and mineralogy for each ash. In Table 1, it can be seen that the % crystallinity from our XRD results and the % crystals from the literature can be different. This indicates that finer ash-sized fractions may have different properties from representative whole-rock samples; thus, in this study we will only consider the % crystallinity and mineralogy that we directly determined by XRD analysis. By comparing Fig. 4 with Table 1, it can be seen that the % crystallinity and % amorphous between ash samples are different, but the S_{ice} onsets are similar. Therefore, the total amount of crystalline vs. amorphous material is likely not the sole factor in determining depositional ice nucleation. Table 2 indicates the detectable crystalline material and their abundances (± 3%). As shown, each of the ash samples contains a considerable amount of plagioclase, either albite, a sodium-rich Na/Ca feldspar, or anorthite, a calcium-rich Na/Ca-feldspar. Feldspar minerals, both K-feldspar and Na/Ca-feldspar, have previously been shown to be among the most efficient depositional ice nuclei, comparable to kaolinite, Arizona

Test Dust, and Mojave Desert Dust (Yakobi-Hancock et al., 2013). Thus, we suggest that Na/Ca-feldspar could be dictating the ice nucleation behavior of volcanic ash. It is important to note that the above discussion only interprets ice nucleation efficiency in terms of a chemical mechanism. The alteration of physical active sites from mechanical grinding or wet generation could increase depositional ice nucleation efficiency; however, our results were comparable to both studies on the Eyjafjallajökull ash, which used dry sieving to size select samples and aerosolized using dry-generation techniques (Steinke et al., 2011;Hoyle et al., 2011).

3.2 Validation of Immersion Freezing Experiments with Kaolinite

To validate our immersion freezing experiments, we have run test experiments on KGa-1b. KGa-1b was chosen because its ice nucleation behavior has been well studied in the immersion freezing mode using both cold stage and continuous flow instruments (Murray et al., 2011;Pinti et al., 2012). Our results for freezing of 10-60 μm droplets containing 1 wt% KGa-1b are shown in Fig. 5. In this experiment, the cumulative fraction of frozen droplets [FF(T)] was determined as a function of temperature:

$$FF(T) = \frac{n_{ice}(T)}{n}, \quad (1)$$

where $n_{ice}(T)$ is the total number of frozen droplets at temperature T and n is the total number of frozen droplets at 233.6 K. Also shown are results for homogeneous freezing of 10-60 μm ultra-pure water droplets from our experimental setup. As expected, the homogeneous freezing curve rises steeply at ~ -37 °C. The droplets containing 1% kaolinite freeze at higher temperatures than the homogeneous freezing curve; thus, the droplets must be freezing heterogeneously. Differences in droplet size bins, ash concentration, and droplet contact angle with the substrate affect both the surface area available for ice nucleation and the subsequent frozen fraction at each temperature. This renders it difficult to directly compare these results to former freezing spectra using different

306 experimental setups. It has, however, been shown in the past that inter-instrumental comparisons
307 of mineral dust can be made by invoking the singular approximation (Vali, 1994, 2008;Broadley
308 et al., 2012;Niemand et al., 2012). Here, the time dependence of freezing events is considered to
309 be of secondary importance to the temperature dependence. In this vein, a simplified quantification
310 of the observed frozen fractions and temperature onsets can be made by the metric of ice nucleation
311 active site (INAS) densities (n_s) (DeMott et al., 1994), which is defined as:

312 $$n_s(T, S_{ice}) = -\frac{\ln[1-FF(T,S_{ice})]}{SA_{aerosol}}, \quad (2)$$

313 where $SA_{aerosol}$ is the average surface area per particle. Our n_s values for KGa-1b as a function of
314 temperature, calculated under the singular description, can be found in Fig. 6a. For $SA_{aerosol}$, the
315 BET specific surface area was used. The BET surface area for KGa-1b was assumed to be 11.8 m^2
316 g^{-1} (Murray et al., 2011). Also shown in Fig. 6a is an n_s parameterization for KGa-1b from Murray
317 et al. (2011), who used a cold stage to determine the immersion freezing potential of KGa-1b for
318 0.2 to 1 wt% solutions using various cooling rates. Our results lie slightly under the Murray
319 parameterization; however, in our analysis we have ignored the time dependence of freezing
320 events. While this may be valid for complex samples with a distribution of ice active sites
321 (Niemand et al., 2012), it has been shown that one must take into account the time dependence for
322 a pure clay mineral like kaolinite (Murray et al., 2011). Despite this, our data analyzed under the
323 singular approximation are only one order of magnitude off from the parameterization. To take
324 into account the time dependence, we invoke the modified singular theory (Vali, 2008). Here, the
325 n_s value is modified to represent a single cooling rate. The parameterization is as follows:

326 $$n_s(T, S_{ice}) = -\frac{\ln[1-FF(T-\alpha,S_{ice})]}{SA_{aerosol}}, \quad (3)$$

327 where the variable α is an offset in temperature from a freezing spectrum recorded at a cooling rate
328 of 1 K min^{-1}. This is related to the cooling rate (r) by the equation

$$\alpha = \beta \log(|r|)\,, \quad (4)$$

where β is an empirical parameter. Our same KGa-1b data parameterized using the modified singular description with β = 2.01 (Murray et al., 2011) can be found in Fig. 6b. Now our data is in excellent agreement with the Murray parameterization. Thus, for immersion freezing, we find that the Raman Microscope cold stage setup can be used to inter-compare inherent immersion freezing abilities of particle types to other instruments under the singular or modified singular approximation. This ability of the Raman Microscope cold stage to determine the inherent immersion freezing ability of NX-Illite nanopowder has also been verified (Hiranuma et al., 2015~~4~~).

3.3 Immersion Freezing of Droplets Containing Volcanic Ash Samples

The immersion freezing results from 0.5, 1.0, and 2.0 wt% Oruanui, Soufrière Hills, and Fuego volcanic ash are shown in Fig. 7. The Oruanui ash samples serve as heterogeneous immersion mode ice nuclei for all wt% explored (Fig. 7a). In general, increasing the wt% of ash in each droplet increases the freezing temperature. This is expected as increasing the wt% of ash in each droplet increases the total surface area available for heterogeneous ice nucleation for a similar-sized droplet population. Although their freezing spectra have different shapes, the temperature at which 50% of 1% Oruanui ash droplets were frozen ($FF_{0.5}$) coincides with the $FF_{0.5}$ of 1 % KGa-1b, indicating that they may have similar immersion freezing abilities. Unlike the depositional freezing results, the immersion freezing activity of the Soufrière Hills ash is not similar to the Oruanui ash (Fig. 7b). In fact, the FF curve for 10-60 µm droplets containing 2 wt% Soufrière Hills ash overlaps with the ultra-pure water curve, implying that these droplets froze homogeneously. Increasing the droplet size range to 65-165 µm only produces a few special IN at T > -37 °C; however, most droplet freezing events still coincide with the homogeneous freezing

curve. For 65-165 µm droplets containing 2 wt% Soufrière Hills ash, the total available surface areas correlate to ash particles with spherical equivalent diameters of 23.0-53.6 µm, which forms a large subset of fine volcanic ash. The Fuego ash has similar immersion freezing behavior to the Soufrière Hills ash, despite coming from a different region and having different silica content (Fig. 7c). Again, for 10-60 µm droplets containing 2 wt% Fuego ash, the FF curve coincides with the homogeneous freezing FF spectrum. Further, for 65-165 µm droplets containing 2 wt% Fuego ash, whose total available surface area corresponded to ash particles 23.4 and 58.0 µm in spherical diameter, only a few special IN at T > -37 °C are found.

Since these ash samples contain different wt% ash, droplet size populations, and ashes with different surface areas, it is difficult to directly compare inherent ice nucleation activity from the freezing spectra. Thus, we have calculated the n_s values for these ash samples under the singular approximation (Fig. 8). For each ash, the BET specific surface area was used as determined in this study (Table 1). The modified singular approximation was not used because larger particle-to-particle variability of ice active sites is expected for these complex samples, limiting the importance of time dependence (Broadley et al., 2012;Hiranuma et al., 2015~~4~~). As shown in Fig. 8, the Oruanui ash is inherently a better ice nuclei than either the Soufrière Hills or Fuego Ash, which are similar to each other. Also shown in Fig. 8 are n_s values of Mt. St. Helens and Eyjafjallajökull ash from previous studies (Hoyle et al., 2011;Steinke et al., 2011;Murray et al., 2012). The Oruanui ash sits below these points; however it should be noted that the surface area of the Eyjafjallajökull and Mt. St. Helens ash were estimated using their geometrical surface area. Due to the high degree of aggregation and porosity of volcanic ash particles, the geometrical surface area could be vastly underestimating the true surface area. To estimate this effect, we have re-plotted the volcanic ash parameterization found in Murray et al. (2012), assuming that the true

surface area is 10 times greater than the estimated geometrical surface area. This is not an unreasonable assumption, since the geometrical surface area would underestimate the true surface area 4-20 times for ash particles 1-5 μm in diameter, assuming a BET surface area for Oruanui ash and a density of 2.6 g m^{-3}. The adjusted parameterization is shown in Fig. 8 as a dashed line. As shown, estimating the surface area as 10 times greater than the geometrical surface area brings the parameterization much closer to our results. Thus, although the Oruanui ash has different surface-area normalized ice nucleation abilities than the Fuego and Soufrière Hills ash used in this study, it appears to be similar to the Eyjafjallajökull and Mt. St. Helens ash.

3.4 Immersion Freezing of Droplets Containing Na/Ca Feldspar

Recently, it has been shown that K-feldspar is an extremely efficient ice nucleus and, consequently, may dictate the ice nucleation ability of natural mineral dust, even though it is only found in low weight percentages (Atkinson et al., 2013). That study also determined the ice nucleation ability of Na/Ca-feldspar from the Bureau of Analysed Samples (United Kingdom), and found that it was also an efficient immersion ice nucleus. In our results, we found that neither the Fuego nor Soufrière Hills ash acted as efficient immersion freezing ice nuclei for the concentrations and droplet sizes that we explored. While the Fuego and Soufrière Hills ash both contained significant feldspar, it was almost exclusively the Na/Ca-feldspar. To explore this further, we conducted immersion freezing experiments on NIST SRM 99b, a Na/Ca-feldspar standard. We also conducted XRD on these samples, and found that they contained K-feldspar and quartz impurities in addition to Na/Ca-Feldspar (Table 2). The frozen fraction curves for NIST SRM 99b are plotted in Fig. 9 and their n_s values are shown in Fig. 8. As shown, the NIST SRM 99b is also an efficient ice nucleus. We suggest that the high immersion freezing activity of the NIST 99b soda feldspar is due to the K-feldspar impurities, in agreement with previous studies

(Atkinson et al., 2013). ~~To our knowledge, a laboratory standard of Na/Ca-feldspar cannot be obtained without these K-feldspar impurities.~~ These combined results suggest that Na/Ca-feldspar may be inactive in the immersion mode despite being very active for depositional nucleation. This is in agreement with Zolles et al. (2015), who found that the Na/Ca-feldspars albite, anorthian andesine, and an albite-dominated ash sample were all weak immersion-mode IN. Thus, from examining Table 2, we suggest that the immersion freezing activity of the Oruanui ash is likely due to the quartz. This is in agreement with previous findings, who found that quartz was the second-most efficient immersion mode nuclei mineral found in mineral dust behind feldspars (Atkinson et al., 2013).

It is important to note that the above discussion interprets immersion freezing only from a chemical mechanism standpoint. The ash samples used here were collected at various distances from the volcano and represent various magnitudes of eruption explosivity, which affects grain morphology and the grain size distribution of the fall deposit, however, it is important to note that these samples were processed prior to immersion freezing. Namely, even after size sorting, the particles were pulverized from larger ash particles and immersed in water and shaken for at least 12 h prior to immersion freezing experiments. Pulverizing the ash particles has two possible effects on ice nucleation. First, it could introduce new, physical active sites. For example it has been shown for hematite particles that mechanical milling can change the ice nucleation surface site density, even when accounting for changes in surface area (Hiranuma et al., 2014). Second, it could liberate and/or expose mineral surfaces that were previously encased in volcanic glass. Both of these effects, however, are expected to increase ice nucleation activity and do not account for the inactivity of the Fuego and Soufrière Hills ashes in the immersion mode. Further, in some cases, approximately 70% of fine ash particles (< 63 μm) are largely aggregates of smaller particles

(Brown et al., 2012). Thus, pulverizing with the Wig-L-Bug® amalgamator may only break apart these aggregates. In the past, it has been shown that wet generation techniques can affect the hygroscopicity and cloud droplet formation ability of mineral dust (Sullivan et al., 2010;Garimella et al., 2014). Thus, allowing the ash samples to shake in solution for at least 12 h prior to immersion freezing experiments could cause the dissolution/redistribution of active surface sites. This, however, is unlikely since this treatment was also conducted for kaolinite, which agrees with previous literature values of wet and dry generated KGa-1b (Pinti et al., 2012;Murray et al., 2011).

4 ATMOSPHERIC IMPLICATIONS

Previously, it has been suggested that all volcanic ash has similar ice nucleation efficiency and may initiate ice below 250-260 K, leading to an overseeding of ice in volcanic plumes (Durant et al., 2008). Since volcanic ash concentration in plumes can be up to 1000 cm^{-3}, overseeding of ice could create a dearth of supercooled water droplets and shut down the Bergeon-Findeisen process, the process of ice crystal growth at the expense of supercooled liquid droplets in mixed-phase clouds. Thus, since particle growth would be reliant on collision processes, overseeding could retard or even prevent the development of precipitation in volcanic plumes. In this work, we have shown that three distinct types of volcanic ash have similar, efficient ice nucleation onsets in the deposition mode. It has been suggested that, large amounts of water in pre-eruptive magma (up to 8% by mass) may render concentration of water in volcanic plumes greater than for typical thunderstorms (McNutt and Williams, 2010). Thus, the primary mode of ice nucleation in volcanic plumes may be immersion freezing. Unlike depositional freezing, the volcanic ash in this study did not possess the same ice nucleation efficiency in the immersion mode; indeed, both the Fuego and Soufrière Hills ash seem inactive in the immersion mode for droplets containing a surface area of ash equivalent to a spherical ash particle ~60 μm in diameter. Thus, our results indicate that

444 some volcanic plumes may not be overseeded with ice. Indeed, this has been directly observed in
445 some volcanic plumes such as the 17 September 1992 eruption of Mt Spurr, where remote sensing
446 measurements showed that ash mass dominated over ice mass (Rose et al., 2001). The current
447 study suggests that immersion freezing, and therefore overseeding, may be dictated by the
448 differences in the mineralogy of the crystalline material found in volcanic ash. Thus, the
449 identification and quantification of mineral phases in fine volcanic ash may be important to
450 correctly predict the many processes in volcanic plumes that rely on ice and hydrometeor
451 formation.

452 It has been shown that ash aggregation, which controls volcanic cloud dispersal, may be reliant
453 on hydrometeor formation (Rose and Durant, 2011). If a volcanic plume is overseeded with ice,
454 hydrometeor growth will be retarded, reducing aggregation and prolonging the lifetime and
455 dispersal of the volcanic cloud (Brown et al., 2012). Correctly modeling volcanic cloud lifetimes
456 and dispersal has important implications for both human health and aviation traffic. Volcanic
457 lightning is another understudied process in volcanic plumes that is thought to be influenced by
458 ice formation (McNutt and Williams, 2010). Volcanic lightning in high-altitude plumes is thought
459 to be produced along a similar mechanism to thundercloud electrification and is important because
460 it represents a hazard and contributes to the global electrification circuit. From this work, we show
461 that some types of ash, depending on their mineralogy, may not initiate ice until the homogeneous
462 freezing limit. Thus, previous thresholds of ice formation in volcanic plumes of 250-260 K may
463 be overestimating the amount of volcanic lightning predicted in models.

464 Volcanic ash also has important climatic implications beyond the initial plume. Fine volcanic
465 ash can stay suspended in the atmosphere for 24 hours and travel 100s to 1000s of km (Brown et
466 al., 2012). Previous work has shown that, while initial plumes contain large concentrations of

water, volcanic clouds can dry out markedly within hours of entering the atmosphere (Schultz et al., 2006). Further, very fine ash can stay suspended much longer than 24 hours and ash fall deposits may remain in local environments for years to decades and can be re-suspended due to human activity (Horwell and Baxter, 2006). In this work, we have shown that all three samples of volcanic ash had similar depositional ice nucleation efficiency (S_{ice} = 1.05 ± 0.01), likely due to Na/Ca-feldspars, which is similar to previous findings on proxies of mineral dust. Thus, since depositional nucleation can occur at lower temperatures than immersion freezing, fine volcanic ash represents a potentially important source of global cold-cloud ice nuclei. Indeed, in one study that took daily measurements of IN concentrations over a 2-year period from central Germany, the highest IN concentrations ever recorded coincided with backwards trajectories of the Eyjafjallajökull volcanic eruption in Iceland (Bingemer et al., 2012). In that same study, the IN concentrations in Israel, over 5000 km away from the source of the eruption, were determined for air-masses originated from the same volcanic eruption. The high IN concentrations found in those air masses were rivaled only during desert dust storms. Electron microscopy measurements confirmed that the most abundant IN in these air masses were volcanic ash. Furthermore, a study using polarization lidars at two central-European stations found a clear influence of volcanic ash on heterogeneous ice nucleation of tropospheric clouds. For example, in that study, all observed cloud layers with cloud top temperatures < -15 °C contained ice during the days following the April 2010 Eyjafjallajökull volcanic eruption (Seifert et al., 2011).

Our experimental results suggest that ice nucleation on fine volcanic ash may exert a non-negligible effect on volcanic plume lifetimes and dynamics as well as on global climate through the formation of cirrus clouds; however, volcanic ice nuclei are currently neglected in global climate models (Hoose et al., 2010). While previous works indicate that a simple parameterization

for all ash types may be possible for the simplification of parameterizing immersion mode volcanic ash ice nuclei in models (Murray et al., 2012), our results indicate that ash types could differ in ice nucleation properties, likely due to their mineralogy. Depositional nucleation on volcanic ash, however, may fall under such a parameterization since all three, distinct ash samples displayed similar depositional ice nucleation onsets to each other and to previous studies on ash from the Eyjafjallajökull volcano (Steinke et al., 2011;Hoyle et al., 2011).

ACKNOWLEDGEMENTS

This work was supported by the National Science Foundation under grants AGS1048536. We thank Bill Rose, Alexa Van Eaton, and the Montserrat Volcano Observatory for the utilized ash samples.

Table 1. Silica content, % crystals from previous whole-rock studies, XRD % crystallinity and % amorphous, and the BET surface areas of representative volcanic rock and ash samples from the Fuego, Soufrière Hills, and Taupo volcanoes and powdered NIST SRM-99b Na/Ca-Feldspar.

Sample	Silica Content (wt%)	% Crystals	XRD % Crystallinity	XRD % Amorphous	BET Surface Area (m^2 g^{-1})
Fuego (Guatemala)	50.6[a]	38 vol%[a]	63 ± 3	37	5.14 ± 0.03
Soufrière Hills (Monserrat)	59.13[b]	60-87 wt%[b]	89 ± 3	11	6.30 ± 0.04
Taupo (Oruanui, New Zealand)	74.15[c]	3-13 wt%[c]	41 ± 3	59	9.23 ± 0.04
Na/Ca-Feldspar (NIST)	-	-	100 ± 3	0	1.219 ± 0.008

[a](Rose et al., 1978)

[b](Murphy et al., 2000)

[c](Wilson et al., 2006)

501

Table 2. The mineralogical composition of Fuego, Soufrière Hills, and Oruanui volcanic ash and NIST SRM-99b Na/Ca-feldspar as determined by XRD.

Mineral/Sample	Anorthite Ca/Na-Feldspar	Albite Na/Ca-Feldspar	Microcline K-Feldspar	Quartz SiO_2	Enstatite Ortho-pyroxene	Riebeckite Magnesio-hornsblende	Other (Trace)
Fuego	36	64	-	-	-	-	-
Soufrière Hills	10	71	-	1	11	7	-
Oruanui	26	47	-	27	-	-	-
Na/Ca-Feldspar (NIST)	-	69	18	13	-	-	Anorthite, Anorthoclase, Barium Silicate Hydrate

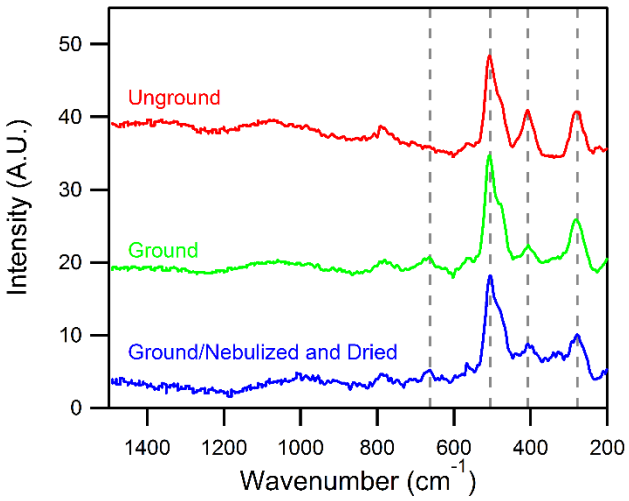

Figure 1. A set of example Raman spectra of unground, ground, and ground/nebulized Soufrière Hills volcanic ash. As shown, the main peaks at 507 cm^{-1}, 408 cm^{-1}, and 281 cm^{-1} (vertical dashed lines) are minimally affected by mechanical grinding and wet generation, suggesting that bulk chemical alteration does not occur. A small peak at 663 cm^{-1}, however, does appear in the ground samples, possibly due to better homogeneity of minor components when compared to unground samples.

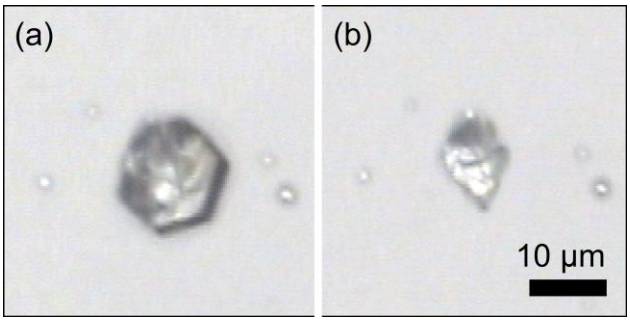

Figure 2. 50x optical image of an ice particle at 225 K (a) and its Fuego ash nucleus (b). ~~The scale bar in the bottom right-hand corner equals 10 µm.~~

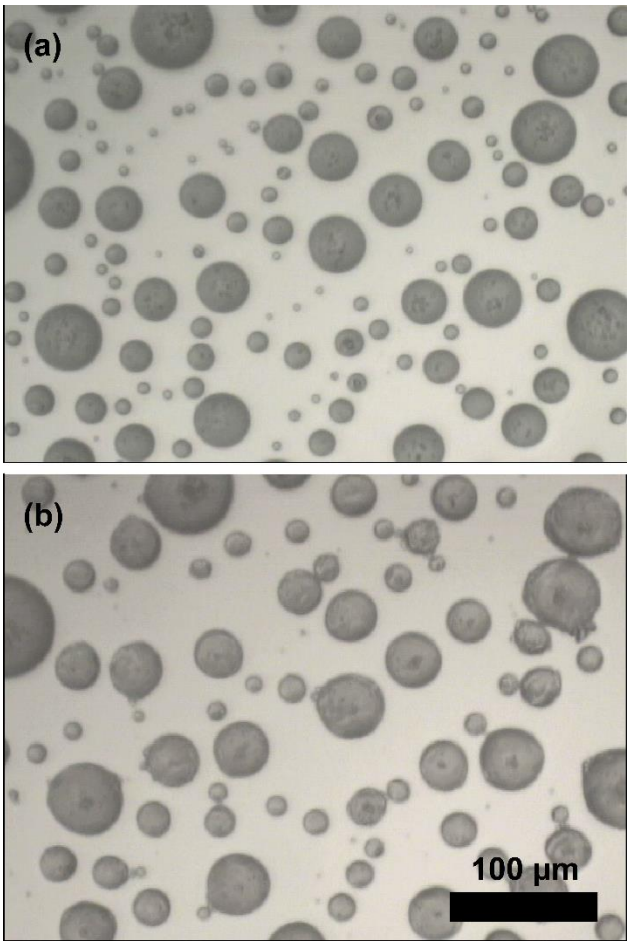

Figure 3. 20x images of unfrozen droplets containing 1% KGa-1b (a), and the same drops after an immersion freezing experiment (b). ~~The scale bar in the bottom right-hand corner equals 100 µm.~~

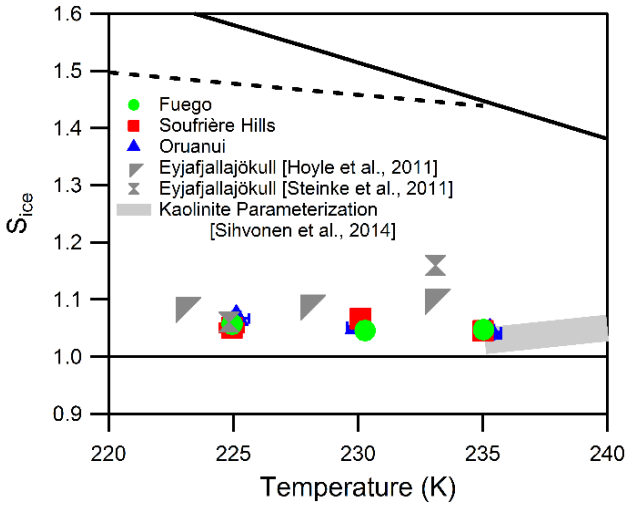

521

522 **Figure 4.** The onset S_{ice} as a function of temperature for nucleation on volcanic ash samples. The
523 thick and thin solid lines refer to water and ice saturation respectively. The dashed line represents
524 the S_{ice} values for homogeneous nucleation of an aqueous droplet (Koop et al., 2000). Also
525 included are onset results from depositional ice nucleation experiments on ash from the 2010
526 Eyjafjallajökull eruption (Hoyle et al., 2011;Steinke et al., 2011) and a parameterization for
527 depositional ice nucleation on KGa-1b (Sihvonen et al., 2014).

528

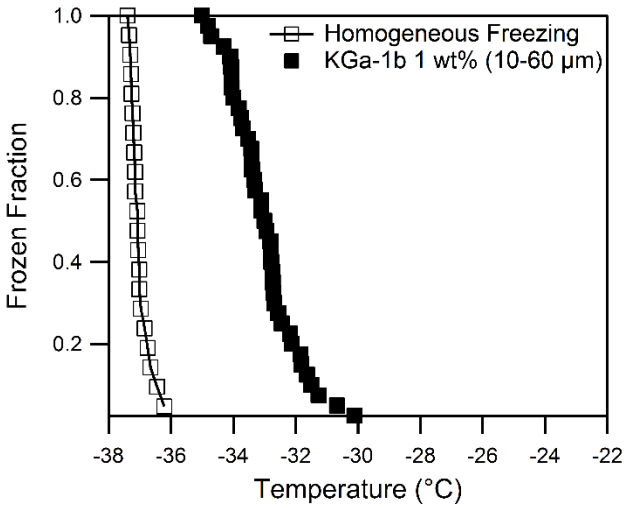

529

530 **Figure 5.** Frozen fraction curve for 1wt% KGa-1b in 10-60 µm droplets as a function of
531 temperature. Also shown are results for freezing of ultra-pure water droplets (homogeneous
532 freezing).

533

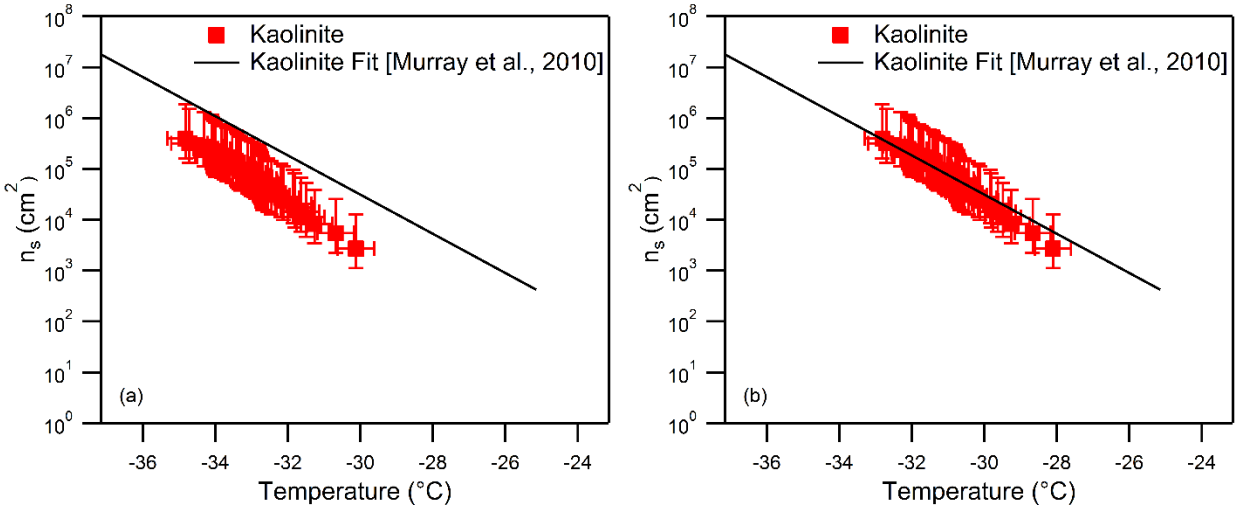

534

535 **Figure 6.** Ice nucleation active surface site densities for KGa-1b as a function of temperature using

536 the singular description (a) and the modified singular description (b).

537

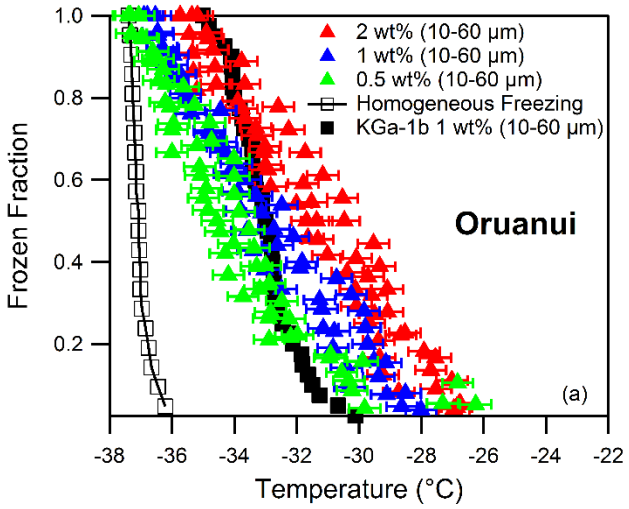
2 wt% (10-60 µm)
1 wt% (10-60 µm)
0.5 wt% (10-60 µm)
Homogeneous Freezing
KGa-1b 1 wt% (10-60 µm)
Oruanui
(a)
Frozen Fraction
Temperature (°C)

538

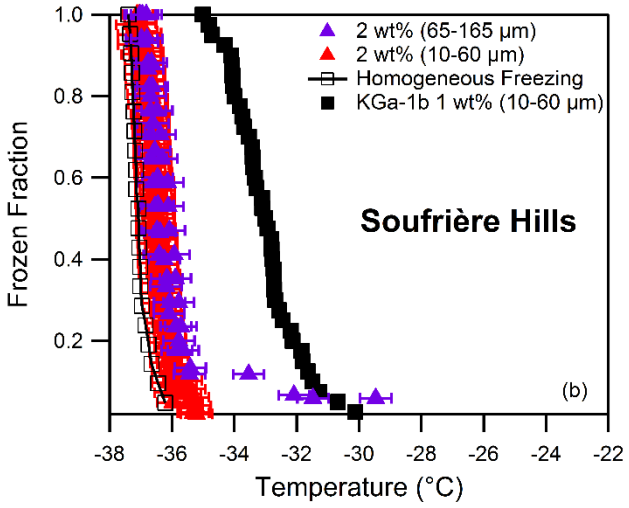
2 wt% (65-165 µm)
2 wt% (10-60 µm)
Homogeneous Freezing
KGa-1b 1 wt% (10-60 µm)
Soufrière Hills
(b)
Frozen Fraction
Temperature (°C)

539

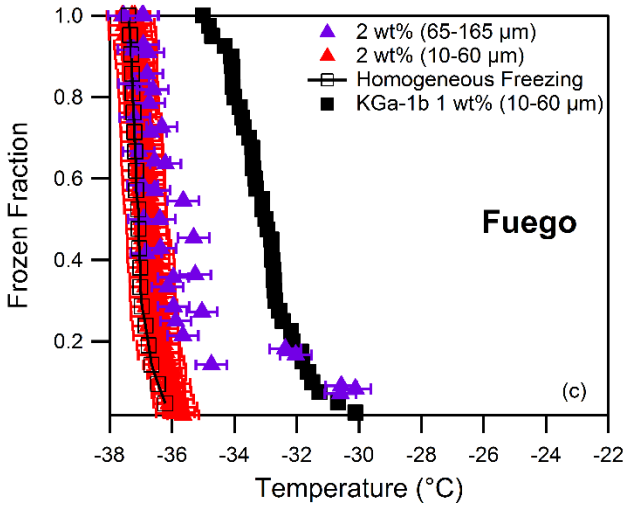
2 wt% (65-165 µm)
2 wt% (10-60 µm)
Homogeneous Freezing
KGa-1b 1 wt% (10-60 µm)
Fuego
(c)
Frozen Fraction
Temperature (°C)

540

Figure 7. Frozen fraction curves as a function of temperature for 0.5, 1.0, and/or 2 wt% Oruanui ash (a), Soufrière Hills (b), and Fuego Ash (c).

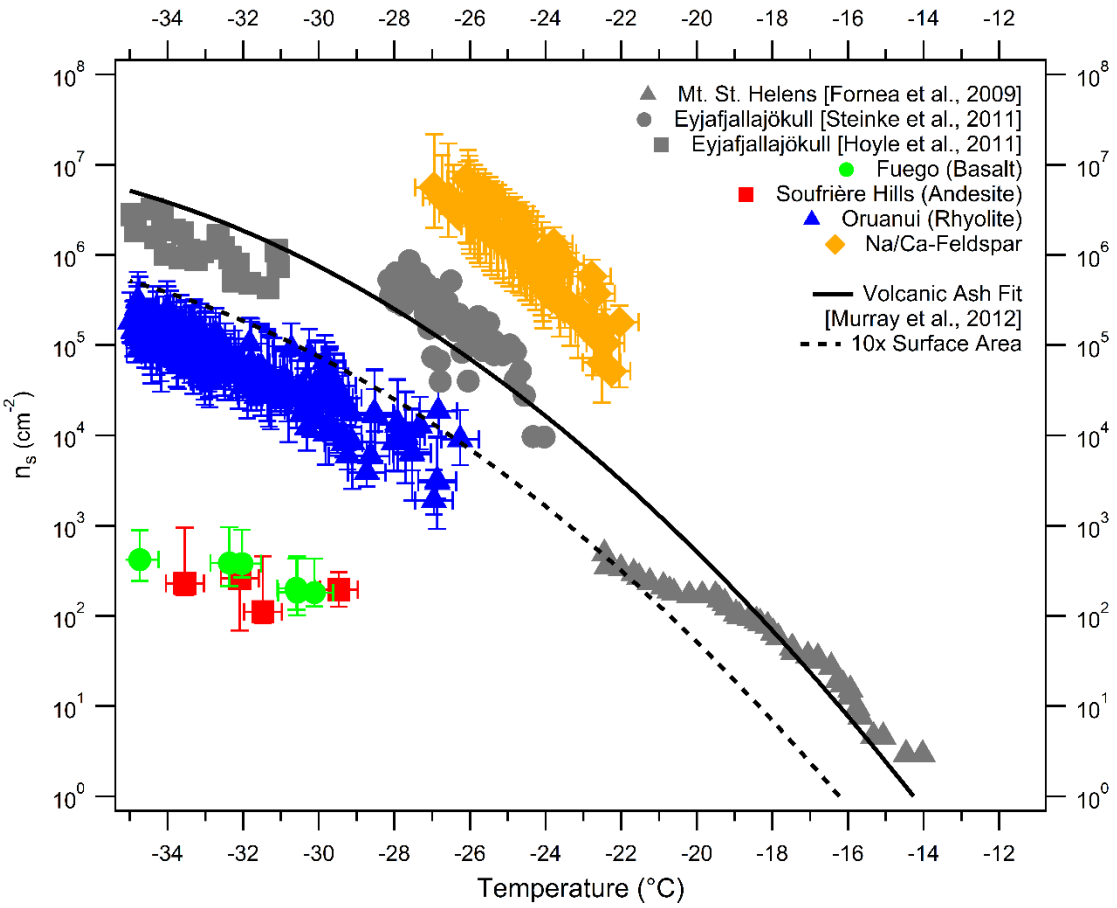

544

545 **Figure 8.** Ice nucleation active surface site densities as a function of temperature for Oruanui,
546 Soufrière Hills, and Fuego ash and NIST SRM-99b Soda Feldspar. Also shown are n_s-values for
547 previous studies (grey markers) on volcanic ash and a parameterization for that data (solid line,
548 (Murray et al., 2012). Additionally, a new parameterization has also been shown that assumes
549 surface area of the volcanic to be 10 times greater than the original parameterization to account for
550 the high porosity of volcanic ash (dashed line).

551

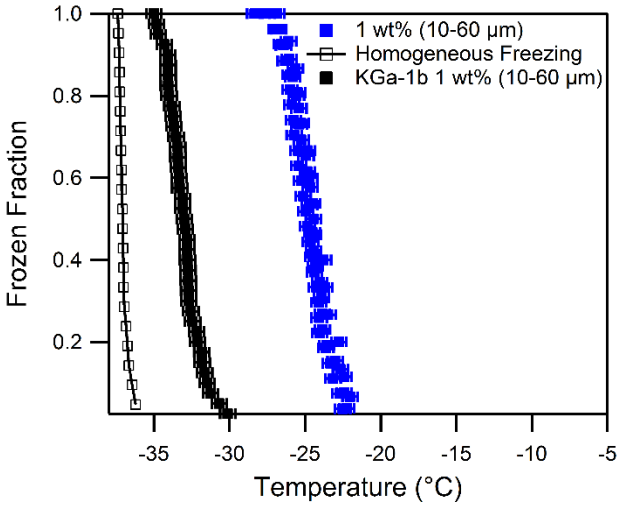

552

553 **Figure 9.** Frozen fraction curve for 1 wt% Na/Ca Feldspar in 10-60 µm droplets as a function of

554 temperature.

555

References

Atkinson, J. D., Murray, B. J., Woodhouse, M. T., Whale, T. F., Baustian, K. J., Carslaw, K. S., Dobbie, S., O'Sullivan, D., and Malkin, T. L.: The importance of feldspar for ice nucleation by mineral dust in mixed-phase clouds, Nature, 498, 355-358, doi:10.1038/nature12278, 2013.

Baustian, K. J., Wise, M. E., and Tolbert, M. A.: Depositional ice nucleation on solid ammonium sulfate and glutaric acid particles, Atmos. Chem. Phys., 10, 2307-2317, doi:10.5194/acp-10-2307-2010, 2010.

Bingemer, H., Klein, H., Ebert, M., Haunold, W., Bundke, U., Herrmann, T., Kandler, K., Mueller-Ebert, D., Weinbruch, S., Judt, A., Weber, A., Nillius, B., Ardon-Dryer, K., Levin, Z., and Curtius, J.: Atmospheric ice nuclei in the Eyjafjallajokull volcanic ash plume, Atmos. Chem. Phys., 12, 857-867, doi:10.5194/acp-12-857-2012, 2012.

Broadley, S. L., Murray, B. J., Herbert, R. J., Atkinson, J. D., Dobbie, S., Malkin, T. L., Condliffe, E., and Neve, L.: Immersion mode heterogeneous ice nucleation by an illite rich powder representative of atmospheric mineral dust, Atmos. Chem. Phys., 12, 287-307, doi:10.5194/acp-12-287-2012, 2012.

Brown, R. J., Bonadonna, C., and Durant, A. J.: A review of volcanic ash aggregation, Phys. Chem. Earth, 45-46, 65-78, doi:10.1016/j.pce.2011.11.001, 2012.

Curtis, D. B., Meland, B., Aycibin, M., Arnold, N. P., Grassian, V. H., Young, M. A., and Kleiber, P. D.: A laboratory investigation of light scattering from representative components of mineral dust aerosol at a wavelength of 550 nm, J. Geophys. Res.-Atmos., 113, D08210, doi:10.1029/2007jd009387, 2008.

DeMott, P. J., Meyers, M. P., and Cotton, W. R.: Parameterization and impact of ice initiation processes relevant to numerical-model simulations of cirrus clouds, J. Atmos. Sci., 51, 77-90, doi:10.1175/1520-0469(1994)051<0077:paioii>2.0.co;2, 1994.

Durant, A. J., Shaw, R. A., Rose, W. I., Mi, Y., and Ernst, G. G. J.: Ice nucleation and overseeding of ice in volcanic clouds, J. Geophys. Res.-Atmos., 113, D09206, doi:10.1029/2007jd009064, 2008.

Durant, A. J., Bonadonna, C., and Horwell, C. J.: Atmospheric and Environmental Impact of Volcanic Particulates, Elements, 6, 235-240, doi:10.2113/gselements.6.4.235, 2010.

Everall, N. J.: Confocal Raman microscopy: common errors and artefacts, Analyst, 135, 2512-2522, doi:10.1039/c0an00371a, 2010.

Fornea, A. P., Brooks, S. D., Dooley, J. B., and Saha, A.: Heterogeneous freezing of ice on atmospheric aerosols containing ash, soot, and soil, J. Geophys. Res.-Atmos., 114, doi:10.1029/2009jd011958, 2009.

Garimella, S., Huang, Y. W., Seewald, J. S., and Cziczo, D. J.: Cloud condensation nucleus activity comparison of dry- and wet-generated mineral dust aerosol: the significance of soluble material, Atmos. Chem. Phys., 14, 6003-6019, doi:10.5194/acp-14-6003-2014, 2014.

Heiken, G.: Morphology and petrography of volcanic ashes, Geological Society of America Bulletin, 83, 1961-1988, doi:10.1130/0016-7606(1972)83[1961:mapova]2.0.co;2, 1972.

Hiranuma, N., Hoffmann, N., Kiselev, A., Dreyer, A., Zhang, K., Kulkarni, G., Koop, T., and Moehler, O.: Influence of surface morphology on the immersion mode ice nucleation efficiency of hematite particles, Atmospheric Chemistry and Physics, 14, 2315-2324, doi:10.5194/acp-14-2315-2014, 2014.

Hiranuma, N., Augustin-Bauditz, S., Bingemer, H., Budke, C., Curtius, J., Danielczok, A., Diehl, K., Dreischmeier, K., Ebert, M., Frank, F., Hoffmann, N., Kandler, K., Kiselev, A., Koop, T., Leisner, T., Möhler, O., Nillius, B., Peckhaus, A., Rose, D., Weinbruch, S., Wex, H., Boose, Y., DeMott, P. J., Hader, J. D., Hill, T. C. J., Kanji, Z. A., Kulkarni, G., Levin, E. J. T., McCluskey, C. S., Murakami, M., Murray, B. J., Niedermeier, D., Petters, M. D., O'Sullivan, D., Saito, A., Schill, G. P., Tajiri, T., Tolbert, M. A., Welti, A., Whale, T. F., Wright, T. P., and Yamashita, K.: A comprehensive laboratory study on the immersion freezing behavior of illite NX particles: a comparison of 17 ice nucleation measurement techniques, Atmos. Chem. Phys., 15, 2489-2518, doi:10.5194/acp-15-2489-2015, 2015.

Hobbs, P. V., Fullerton, C.M, and Bluhm, G. C.: ICE NUCLEUS STORMS IN HAWAII, Nat.-Phys. Sci., 230, 90-1, 1971.

Hoose, C., Kristjansson, J. E., Chen, J.-P., and Hazra, A.: A Classical-Theory-Based Parameterization of Heterogeneous Ice Nucleation by Mineral Dust, Soot, and Biological Particles in a Global Climate Model, J. Atmos. Sci., 67, 2483-2503, doi:10.1175/2010jas3425.1, 2010.

Hoose, C., and Moehler, O.: Heterogeneous ice nucleation on atmospheric aerosols: a review of results from laboratory experiments, Atmos. Chem. Phys., 12, 9817-9854, doi:10.5194/acp-12-9817-2012, 2012.

Horwell, C. J., and Baxter, P. J.: The respiratory health hazards of volcanic ash: a review for volcanic risk mitigation, B. Volcanol., 69, 1-24, doi:10.1007/s00445-006-0052-y, 2006.

Hoyle, C. R., Pinti, V., Welti, A., Zobrist, B., Marcolli, C., Luo, B., Hoeskuldsson, A., Mattsson, H. B., Stetzer, O., Thorsteinsson, T., Larsen, G., and Peter, T.: Ice nucleation properties of volcanic ash from Eyjafjallajokull, Atmos. Chem. Phys., 11, 9911-9926, doi:10.5194/acp-11-9911-2011, 2011.

623 Hudson, P. K., Gibson, E. R., Young, M. A., Kleiber, P. D., and Grassian, V. H.: Coupled
624 infrared extinction and size distribution measurements for several clay components of mineral dust
625 aerosol, J. Geophys. Res.-Atmos., 113, D011201, doi:10.1029/2007jd008791, 2008.

626 Huneeus, N., Schulz, M., Balkanski, Y., Griesfeller, J., Prospero, J., Kinne, S., Bauer, S.,
627 Boucher, O., Chin, M., Dentener, F., Diehl, T., Easter, R., Fillmore, D., Ghan, S., Ginoux, P.,
628 Grini, A., Horowitz, L., Koch, D., Krol, M. C., Landing, W., Liu, X., Mahowald, N., Miller, R.,
629 Morcrette, J. J., Myhre, G., Penner, J., Perlwitz, J., Stier, P., Takemura, T., and Zender, C. S.:
630 Global dust model intercomparison in AeroCom phase I, Atmos. Chem. Phys., 11, 7781-7816,
631 doi:10.5194/acp-11-7781-2011, 2011.

632 Isono, K., Komabayasi, M., and Ono, A.: Volcanoes as a source of atmospheric ice nuclei,
633 Nature, 183, 317-318, doi:10.1038/183317a0, 1959.

634 Kolb, C. E., Cox, R. A., Abbatt, J. P. D., Ammann, M., Davis, E. J., Donaldson, D. J.,
635 Garrett, B. C., George, C., Griffiths, P. T., Hanson, D. R., Kulmala, M., McFiggans, G., Poschl,
636 U., Riipinen, I., Rossi, M. J., Rudich, Y., Wagner, P. E., Winkler, P. M., Worsnop, D. R., and O'
637 Dowd, C. D.: An overview of current issues in the uptake of atmospheric trace gases by aerosols
638 and clouds, Atmos. Chem. Phys., 10, 10561-10605, doi:10.5194/acp-10-10561-2010, 2010.

639 Koop, T., Ng, H. P., Molina, L. T., and Molina, M. J.: A new optical technique to study
640 aerosol phase transitions: The nucleation of ice from H2SO4 aerosols, J. Phys. Chem. A, 102,
641 8924-8931, doi:10.1021/jp9828078, 1998.

642 Koop, T., Luo, B. P., Tsias, A., and Peter, T.: Water activity as the determinant for
643 homogeneous ice nucleation in aqueous solutions, Nature, 406, 611-614, doi:10.1038/35020537,
644 2000.

645 Langer, G., Garcia, C. J., Mendonca, B. G., Pueschel, R. F., and Fullerton, C.M.: Hawaiian
646 volcanos—source of ice nuclei, J. Geophys. Res., 79, 873-875, doi:10.1029/JC079i006p00873,
647 1974.

648 Langmann, B.: On the Role of Climate Forcing by Volcanic Sulphate and Volcanic Ash,
649 Adv. Meteorol., 340123, doi:10.1155/2014/340123, 2014.

650 McNutt, S. R., and Williams, E. R.: Volcanic lightning: global observations and constraints
651 on source mechanisms, B. Volcanol., 72, 1153-1167, doi:10.1007/s00445-010-0393-4, 2010.

652 Murphy, D. M., and Koop, T.: Review of the vapour pressures of ice and supercooled water
653 for atmospheric applications, Q. J. Roy. Meteorol. Soc., 131, 1539-1565, doi:10.1256/qj.04.94,
654 2005.

Murphy, M. D., Sparks, R. S. J., Barclay, J., Carroll, M. R., and Brewer, T. S.: Remobilization of andesite magma by intrusion of mafic magma at the Soufriere Hills Volcano, Montserrat, West Indies, J. Petrol., 41, 21-42, doi:10.1093/petrology/41.1.21, 2000.

Murray, B. J., Broadley, S. L., Wilson, T. W., Atkinson, J. D., and Wills, R. H.: Heterogeneous freezing of water droplets containing kaolinite particles, Atmos. Chem. Phys., 11, 4191-4207, doi:10.5194/acp-11-4191-2011, 2011.

Murray, B. J., O'Sullivan, D., Atkinson, J. D., and Webb, M. E.: Ice nucleation by particles immersed in supercooled cloud droplets, Chem. Soc. Rev., 41, 6519-6554, doi:10.1039/c2cs35200a, 2012.

Niemand, M., Moehler, O., Vogel, B., Vogel, H., Hoose, C., Connolly, P., Klein, H., Bingemer, H., DeMott, P., Skrotzki, J., and Leisner, T.: A Particle-Surface-Area-Based Parameterization of Immersion Freezing on Desert Dust Particles, J. Atmos. Sci., 69, 3077-3092, doi:10.1175/jas-d-11-0249.1, 2012.

Pinti, V., Marcolli, C., Zobrist, B., Hoyle, C. R., and Peter, T.: Ice nucleation efficiency of clay minerals in the immersion mode, Atmos. Chem. Phys., 12, 5859-5878, doi:10.5194/acp-12-5859-2012, 2012.

Robock, A.: Climatic Impact of Volcanic Emissions, in: The State of the Planet: Frontiers and Challenges in Geophysics, American Geophysical Union, Washington, D.C., 125-134, 2004.

Rose, W. I., Anderson, A. T., Woodruff, L. G., and Bonis, S. B.: October 1974 basaltic tephra from fuego volcano—description and history of magma body, J. Volcanol. Geoth. Res., 4, 3-53, doi:10.1016/0377-0273(78)90027-6, 1978.

Rose, W. I., Bluth, G. J. S., Schneider, D. J., Ernst, G. G. J., Riley, C. M., Henderson, L. J., and McGimsey, R. G.: Observations of volcanic clouds in their first few days of atmospheric residence: The 1992 eruptions of Crater Peak, Mount Spurr volcano, Alaska, J. Geol., 109, 677-694, doi:10.1086/323189, 2001.

Rose, W. I., and Durant, A. J.: Fate of volcanic ash: Aggregation and fallout, Geology, 39, 895-896, doi:10.1130/focus092011.1, 2011.

Schill, G. P., and Tolbert, M. A.: Heterogeneous ice nucleation on phase-separated organic-sulfate particles: effect of liquid vs. glassy coatings, Atmos. Chem. Phys., 13, 4681-4695, doi:10.5194/acp-13-4681-2013, 2013.

Schnell, R. C., and Delany, A. C.: Airborne ice nuclei near an active volcano, Nature, 264, 535-536, doi:10.1038/264535a0, 1976.

687 Schultz, D. M., Kanak, K. M., Straka, J. M., Trapp, R. J., Gordon, B. A., Zrnic, D. S.,
688 Bryan, G. H., Durant, A. J., Garrett, T. J., Klein, P. M., and Lilly, D. K.: The mysteries of
689 mammatus clouds: Observations and formation mechanisms, J. Atmos. Sci., 63, 2409-2435,
690 doi:10.1175/jas3758.1, 2006.

691 Seifert, P., Ansmann, A., Gross, S., Freudenthaler, V., Heinold, B., Hiebsch, A., Mattis, I.,
692 Schmidt, J., Schnell, F., Tesche, M., Wandinger, U., and Wiegner, M.: Ice formation in ash-
693 influenced clouds after the eruption of the Eyjafjallajokull volcano in April 2010, J. Geophys.
694 Res.-Atmos., 116, doi:10.1029/2011jd015702, 2011.

695 Sihvonen, S. K., Schill, G. P., Lyktey, N. A., Veghte, D. P., Tolbert, M. A., and Freedman,
696 M. A.: Chemical and Physical Transformations of Aluminosilicate Clay Minerals Due to Acid
697 Treatment and Consequences for Heterogeneous Ice Nucleation, J. Phys. Chem. A, 118, 8787-
698 8796, doi:10.1021/jp504846g, 2014.

699 Small, C., and Naumann, T.: The global distribution of human population and recent
700 volcanism, Environ. Hazards, 3, 93-109, doi:10.3763/ehaz.2001.0309, 2001.

701 Steinke, I., Moehler, O., Kiselev, A., Niemand, M., Saathoff, H., Schnaiter, M., Skrotzki,
702 J., Hoose, C., and Leisner, T.: Ice nucleation properties of fine ash particles from the
703 Eyjafjallajokull eruption in April 2010, Atmos. Chem. Phys., 11, 12945-12958, doi:10.5194/acp-
704 11-12945-2011, 2011.

705 Sullivan, R. C., Moore, M. J. K., Petters, M. D., Kreidenweis, S. M., Qafoku, O., Laskin,
706 A., Roberts, G. C., and Prather, K. A.: Impact of Particle Generation Method on the Apparent
707 Hygroscopicity of Insoluble Mineral Particles, Aerosol Sci. Tech., 44, 830-846,
708 doi:10.1080/02786826.2010.497514, 2010.

709 Todoli, J. L., and Mermet, J. M.: Liquid Sample Introduction in ICP Spectrometry: A
710 Practical Guide, Elsevier Science, the Netherlands, 2011.

711 Vali, G., and Stansbury, E. J.: Time-dependent characteristics of heterogeneous nucleation
712 of ice, Can. J. Phys., 44, 477-502, 1966.

713 Vali, G.: Freezing rate due to heterogeneous nucleation, J. Atmos. Sci., 51, 1843-1856,
714 doi:10.1175/1520-0469(1994)051<1843:frdthn>2.0.co;2, 1994.

715 Vali, G.: Repeatability and randomness in heterogeneous freezing nucleation, Atmos.
716 Chem. Phys., 8, 5017-5031, doi:10.5194/acp-8-5017-2008, 2008.

717 Van Eaton, A. R., Muirhead, J. D., Wilson, C. J. N., and Cimarelli, C.: Growth of volcanic
718 ash aggregates in the presence of liquid water and ice: an experimental approach, B. Volcanol.,
719 74, 1963-1984, doi:10.1007/s00445-012-0634-9, 2012.

Wilson, C. J. N., Blake, S., Charlier, B. L. A., and Sutton, A. N.: The 26.5 ka Oruanui eruption, Taupo volcano, New Zealand: Development, characteristics and evacuation of a large rhyolitic magma body, J. Petrol., 47, 35-69, 2006.

Wise, M. E., Baustian, K. J., and Tolbert, M. A.: Internally mixed sulfate and organic particles as potential ice nuclei in the tropical tropopause region, P. Natl. Acad. Sci. USA, 107, 6693-6698, doi:10.1073/pnas.0913018107, 2010.

Witham, C. S., Oppenheimer, C., and Horwell, C. J.: Volcanic ash-leachates: a review and recommendations for sampling methods, J. Volcanol. Geoth. Res., 141, 299-326, doi:10.1016/j.jvolgeores.2004.11.010, 2005.

Yakobi-Hancock, J. D., Ladino, L. A., and Abbatt, J. P. D.: Feldspar minerals as efficient deposition ice nuclei, Atmos. Chem. Phys., 13, 11175-11185, doi:10.5194/acp-13-11175-2013, 2013.

Zolles, T., Burkart, J., Häusler, T., Pummer, B., Hitzenberger, R., and Grothe, H.: Identification of Ice Nucleation Active Sites on Feldspar Dust Particles, J. Phys. Chem. A, 119, 2692-2700, doi:10.1021/jp509839x, 2015.